

Intelligent Control to Suppress Epileptic Seizures in the Amygdala: In Silico Investigation Using a Network of Izhikevich Neurons

Gabriel da Silva Lima[®], *Member, IEEE*, Vinícius Rosa Cota[®], and Wallace Moreira Bessa[®], *Senior Member, IEEE*

Abstract—Closed-loop electrical stimulation of brain structures is one of the most promising techniques to suppress epileptic seizures in drug-resistant refractory patients who are also ineligible to ablative neurosurgery. In this work, an intelligent controller is presented to block the aberrant activity of a network of Izhikevich neurons of three different types, used here to model the electrical activity of the basolateral amygdala during ictogenesis, i.e. its transition from asynchronous to hypersynchronous state. A Lyapunov-based nonlinear scheme is used as the main framework for the proposed controller. To avoid the issue of accessing each neuron individually, local field potentials are used to gain insight into the overall state of the Izhikevich network. Artificial neural networks are integrated into the control scheme to manage unknown dynamics and disturbances caused by brain electrical activity that are not accounted for in the model. Four different cases of ictogenesis induction were tested. The results show the efficacy of the proposed control strategy to suppress epileptic seizures and suggest its capability to address both patient-specific and patient-to-patient variability.

Index Terms—Epilepsy, amygdala, seizure suppression, intelligent control, artificial neural networks.

I. INTRODUCTION

EUROLOGICAL disorders, including epilepsy, motor impairments, and neuropsychiatric dysfunctions, continue to be a significant contributor to adult-onset disability on a global scale [1], [2]. Moreover, primary treatments like pharmacotherapy, neurosurgery, or physical therapy often fall

Received 24 September 2024; revised 19 January 2025 and 5 February 2025; accepted 17 February 2025. Date of publication 19 February 2025; date of current version 26 February 2025. This work was supported by the Brazilian Research Agencies Conselho Nacional de Desenvolvimento Científico e Tecnológico (CNPq) and Coordenação de Aperfeiçoamento de Pessoal de Nível Superior (CAPES). The work of Gabriel da Silva Lima was supported by the Brazilian Coordination for the Improvement of Higher Education Personnel. (Corresponding author: Wallace Moreira Bessa.)

Gabriel da Silva Lima and Wallace Moreira Bessa are with the Smart Systems Laboratory, University of Turku, 20520 Turku, Finland (e-mail: gdasil@utu.fi; wmobes@utu.fi).

Vinícius Rosa Cota is with the Rehab Technologies Laboratory, Istituto Italiano di Tecnologia, 16163 Genoa, Italy (e-mail: vinicius.rosacota@iit.it).

Digital Object Identifier 10.1109/TNSRE.2025.3543756

short in providing complete symptom relief or substantial recovery of neural function. For example, in the case of epilepsy, in circa one-third of the patients, seizures are resistant to anti-epileptic drugs [3]. Among this group, approximately 35% are ineligible for neurosurgical methods [4]. Given the widespread prevalence of the disease (affecting 1-2% of the global population), these values translate into millions of individuals grappling with uncontrollable seizures [5], [6].

Since the beginning of the last century, the neuroscience community has investigated technologies to connect the brain and electro-electronic devices, aiming to regulate and correct abnormal brain activity for potential symptom relief, full recovery, and even a cure. Referred to broadly as neurotechnologies, this multifaceted approach encompasses decoding descriptive signals from the brain and manipulating neuronal cell activity by directly applying stimuli of various physical forms, effectively bypassing somatosensory neural functions. Among the diverse possibilities, electrophysiological interfaces emerge as the most extensively developed and widely used, playing crucial roles in both experimental and clinical settings. Electrical stimulation, particularly, has undergone significant advancements in the last 50 years propelled by progress in neuroscientific knowledge, neurosurgery, and digital technology [7]. Recent breakthroughs, such as disruptive neuronal sensor technology, large-scale integration of electronic circuits, machine learning techniques, and neuromorphism, herald a new phase in the field, marked by a major paradigm shift like closed-loop approaches [8], [9]. Despite such substantial progress, the predominant approach in clinical or experimental applications involves neurotechnology operating in an open-loop circuit, in which neural stimulation adheres to a fixed set of parameters, only changing through expert intervention.

In simple open-loop mode of operation, electrophysiological recordings come into play either before stimulation for diagnostic purposes or after treatment to evaluate the therapeutic efficacy of neuromodulation. Conversely, closed-loop neuroengineering systems, such as illustrated by Fig. 1(a), where stimulation is directly controlled in real time by means of electrophysiological data, has been proven superior. This dynamic approach responds to the non-stationary nature of

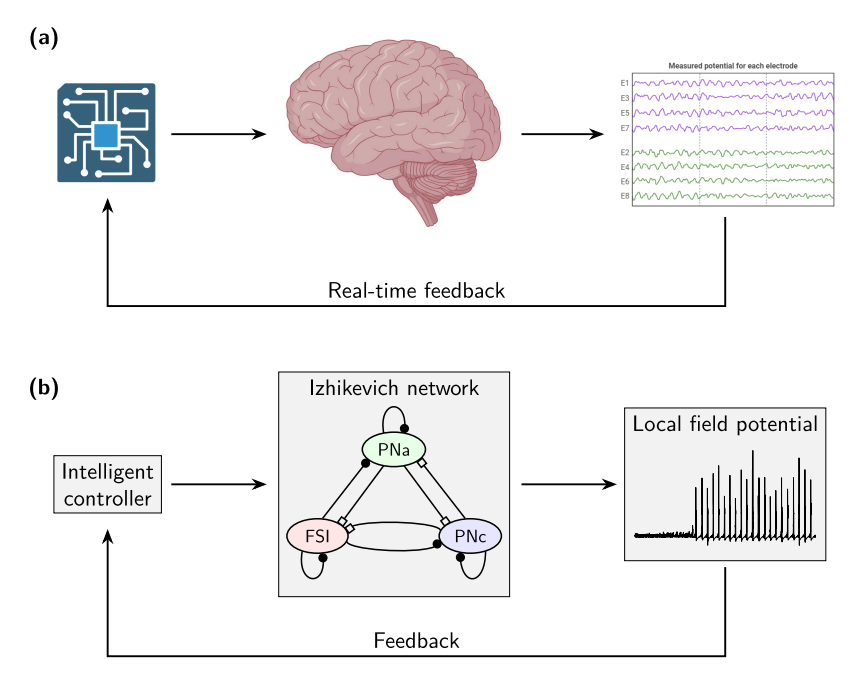


Fig. 1. Framework of feedback control applied to neuroengineering: (a) representation of an actual feedback control process, where electrical signals obtained by electrodes are used to calculate the electrical stimulus to be applied to the brain; (b) proposed simulation scheme for feedback control in which the Izhikevich network emulates the behavior of a brain portion, the basolateral amygdala, and the local field potential (LFP) is used as input to the intelligent controller.

brain activity, identifying optimal timeframes for stimulus delivery and allowing fine-tuning of parameters. Hence, this results in increased efficacy (resulting in a stronger therapeutic result) and efficiency (delivering stimulation only when required) [10].

To implement closed-loop neuroengineering systems, the development of computational and mathematical strategies capable of connecting features of electrophysiological recordings to electrical stimulation parameters in real time is imperative. This crucial step ensures the seamless closure of the loop, allowing for dynamic responsiveness to the intricate nature of brain activity. Wagenaar et al. [11], for example, proposed a feedback adaptive scheme based on neuron firing rate to manipulate the stimulation voltage applied to a neocortical cell culture of rats. da Silva Lima et al. [12] proposed a reinforcement learning algorithm to optimize the pulse frequency of an electrical stimulus. Liang et al. [13] and Rouhani et al. [14] presented interesting simulation results by applying model-based closed-loop strategies for suppressing seizures in abstract models such as the Epileptor and Jansen-Rit model [13] and biological conductance-based models of Hodgkin-Huxley (HH model) [14]. Koppert et al. [15] applied target stimulation to postpone epileptic seizures in a network of HH neurons. More applications of closed-loop strategies to suppress or detect epileptiform activity can be found on [16], [17], [18], and [19].

Beyond the issue of how the control signal is applied, it is worth raising another important matter: the fact that neurostimulation may be successful with one patient does not guarantee that it will work with another. The success of the chosen control approach can depend on several factors, such as age, gender, genetics, anatomical variability, etc. [20],

[21]. Therefore, it is crucial that the design of the control approach takes into account the possibility of parametric unpredictability and variability among patients, enabling automatic personalized-like neurostimulation approaches.

In this context, intelligent control can be a suitable choice for a closed-loop technique with the goal of suppressing epileptic seizures. By the combination of nonlinear control approaches with computational intelligence schemes, the controller can stabilize the patient condition while it estimates, compensates and/or rejects the epileptiform activity as well as the occasional external influences from other brain regions. Intelligent controllers are widely adopted to control mechatronic/mechanic systems such as underwater vehicles [22], [23], [24], robots [25], [26], overhead cranes [27], [28], among other applications [29], [30], [31], [32]. In the last years, intelligent controllers have also been applied to bio-systems in order to regulate vital signals such as cardiac rhythms [33], [34] and blood glucose levels [35]. In such cases, the controller was able not only to compensate for interpatient variability, with the intelligent approach addressing different cases of cardiac diseases [34], but also to manage intrapatient fluctuation when different scenarios of food intake were considered in the control of glucose concentration [35]. Regarding intelligent control applied to suppress seizure events related to epilepsy, Narayanan and Subbian [36] applied Model Predictive Control with recurrent neural networks for a network of neurons based on the HH model. Bessa and Lima [37] have applied a feedback linearization approach with neural networks for electric circuit of memristors based on the neuronal HH model for suppression of seizure-like events. It is important to highlight that the HH models are known to be computationally expensive to implement, specially networks of thousands of neurons [38]. It is also worth to mention the work of Brogin et al. [39] who applied feedback linearization with a fuzzy Takagi-Sugeno model for suppressing epileptic seizures of a neural dynamics reproduced by an Epileptor model [40].

In this work, we propose a Lyapunov-based nonlinear control approach as the main framework of an intelligent controller to diminish or even suppress the ictogenesis process in a network of neurons. To achieve that, we employed adaptive neural networks to deal with modeling inaccuracies and external disturbances, such as background activity from other neurons. To ensure safe applications, the boundedness and convergence properties of the closed-loop signals are rigorously proved by means of a Lyapunov-like stability analysis even when no prior knowledge of the mathematical model is assumed. Overall, the main advantages of the proposed controller are presented below:

- the selected configuration of the artificial neural network (ANN) requires just one hidden layer and a single neuron in the input, rather than encompassing all system states or state errors. This choice significantly reduces the computational complexity of the neural network, making its integration into low-power microcontrollers far more feasible;
- by utilizing online learning to update the ANN weights, as opposed to supervised offline training, the adopted neural network can consistently learn and approximate neuronal activity over time;
- 3) no prior knowledge about the system to be controlled is required, which allows it to adapt to different epileptic trigger scenarios.

Based on the points presented above, it is worth high-lighting that the proposed controller framework has four key conceptual features: (1) the neural estimator functions as a predictive tool by incorporating model dynamics and anticipating the estimation action used in the controller; (2) the online updating process allows the ANN to adapt to changes in the system; (3) through continuous online learning, the controller incorporates knowledge about the system, enhancing prediction and adaptation processes and enabling it to handle intra-individual variability and structural anatomical diversity among patients; and (4) because the controller is designed through a Lyapunov-like stability analysis, it is robust against modeling uncertainties and external influences. Therefore, the proposed controller meets the criteria presented by Bessa et al. [41] for biologically inspired intelligent control.

A network of Izhikevich neurons is used to model the Amygdala region, highly important in epileptic phenomena and neuromodulation treatments [42], [43]. Synaptic weights of the network were gradually increased to simulate seizure development, or the transition from asynchronous to hypersynchronous state, in a computational environment. It is important to clarify that our control objective is to regulate the overall state of the Izhikevich network rather than controlling individual neurons in isolation. Controlling each neuron independently would be impractical, as it would require not only monitoring the behavior of every neuron but also delivering precise electrical stimuli to each one. In this regard, we calculated approximations of local field potentials of the

simulated network to identify irregular neural activity patterns and responsively administered electrical stimulation into the model to regulate it, as illustrated in Fig. 1(b). To access each neuron, the control signal is scaled by a factor representing the distance between the probe and the neuron within the pool.

The remainder of the article is organized as follows: Section II introduces the model of the Izhikevich neuronal network; Section III details the proposed intelligent controller; Section IV presents the simulation results; and finally, our concluding remarks are presented in section V.

II. NEURONAL MODEL OF THE AMYGDALA

The main mode of communication between neurons is by sudden and temporary changes in membrane voltage that travel via the axon until the synaptic cleft where the signal is transmitted neurochemically to affect other neurons. This is called an action potential or, simply, a neuronal spike, as shown in Fig. 2(a). To represent the dynamical behavior of a network of true biological neurons, it is important that the model be able to accurately reproduce the cells' characteristic firing patterns. Izhikevich [44] proposed a nonlinear integrate-and-fire model that effectively captures such variability, demonstrating its biophysical validity and suitability for large-scale simulations. In this context, the basolateral amygdala model, Fig. 2(b), is constructed by a network of different types of Izhikevich neurons [45], [46]. Therefore, the model that represents the membrane potential for each neuron is described by the following set of equations:

$$\dot{\mathbf{v}} = 0.04 \ D_v \mathbf{v} + 5\mathbf{v} + 140 - \mathbf{u} + \mathbf{I} - \mathbf{J} \tag{1}$$

$$\dot{\boldsymbol{u}} = a(D_h \boldsymbol{v} - \boldsymbol{u}) \tag{2}$$

if
$$v_k \ge 30$$
 mV, then
$$\begin{cases} v_k \leftarrow c_k \\ u_k \leftarrow u_k + d_k \end{cases}$$
 (3)

in which $v \in \mathbb{R}^N$ represents the membrane potential of the neuron, $u \in \mathbb{R}^N$ stands for a membrane recovery variable, $D_h \in \mathbb{R}^{N \times N}$ is the diagonal matrix with h_k elements, where h = v, b, I denotes the synaptic currents, and J the injected current. Furthermore, the parameter a scales the recovery variable's time, b describes the sensitivity of u, c is the resting potential of v, and d describes the reset of u after firing.

The cytoarchitecture, similar to that of the basolateral amygdala, region of the human brain with approximately 11 million neurons [47], must accurately depict the predominant cell type distribution within this area and exhibit firing patterns and oscillations characteristic of both synchronous and asynchronous forebrain states [38], [46], [48]. Therefore, following the proportions provided by Feng et al. [46] and considering a network of N = 1200 neurons, the population is composed by $N_a = 768 (64\%)$ of principal neuronal cells with adaptation (PNa), $N_c = 312$ (26%) of principal neuronal cells with continuous spiking (PNc), and $N_I = 120$ (10%) of fastspiking inhibitory neurons (FSI). These cells were assigned with the firing patterns typically observed in electrophysiological recordings in the basolateral amygdala. The excitatory neurons, specifically PNa and PNc, were assigned the firing patterns of regular spiking (RS) and chattering (CH) neurons, respectively. In turn, the inhibitory neurons (FSI) replicated the

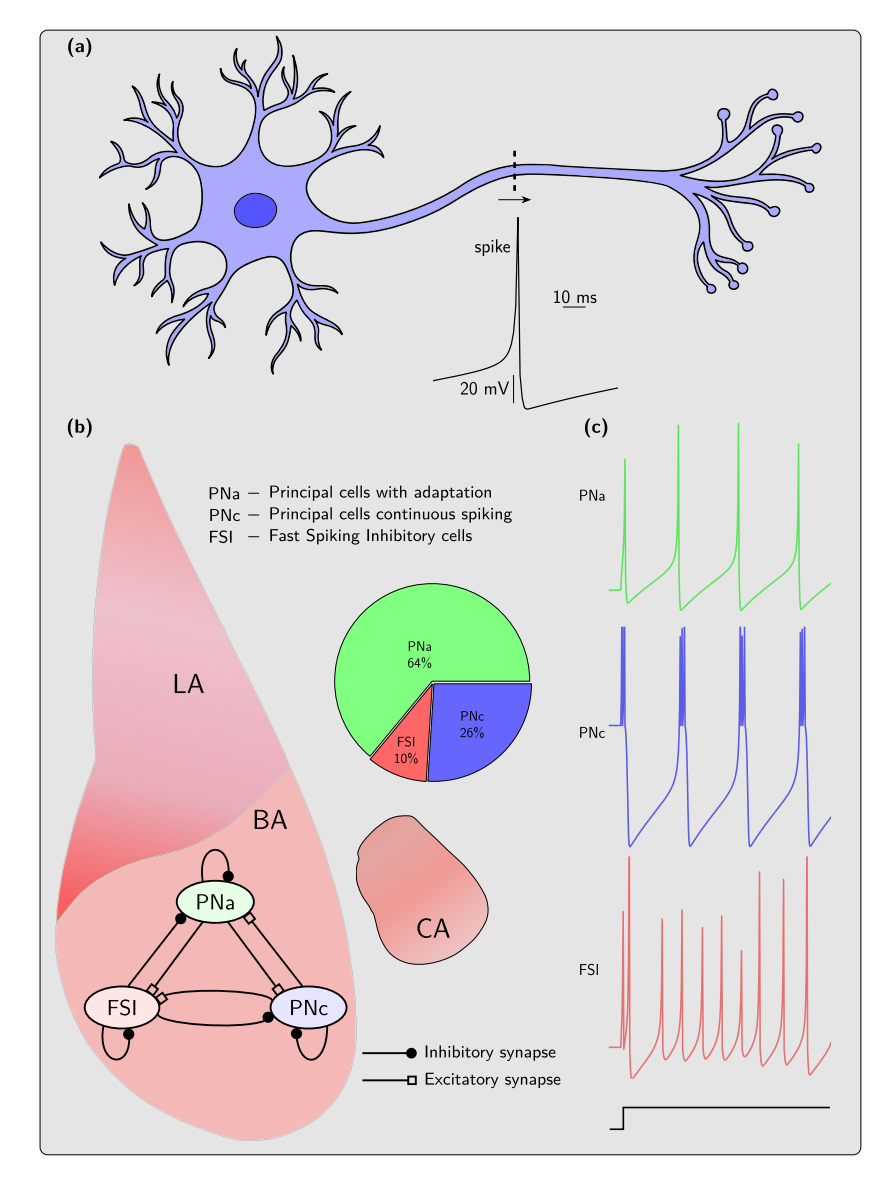


Fig. 2. Basolateral Amygdala (BA) model. The neural model is based on Izhikevich representation for spiking neurons. The spikes (abrupt and transient changes of membrane potential propagated along the axon to other neurons) are the principal means of communication between neurons. The implemented network is formed of 768 main cells with adaptation (PNa), 312 neurons with continuous spiking (PNc), and 120 fast spiking inhibitory neurons (FSI). This network was made to be recurrent with all-to-all connections, where PNa, PNc and FSI were connected among themselves and with each other. LA: lateral amygdala; CA: central amygdala.

low-threshold spiking (LTS) neurons [38], [44]. The distinctive pattern of each neuron type is shown in Fig. 2(c). The network is full-connected by the matrix of synaptic weights $S \in \mathbb{R}^{N \times N}$, where each s_{mn} weight is obtained from a continuous uniform distribution with amplitude 0.5 for the PNa and PNc neurons and -3.5 for the FSI.

This work considered the initial states of v and u as being $v_0 = c$ mV and $u_0 = D_b v_0$ mV. The parameters are defined as follows:

$$\begin{array}{l} D_{b,k} = 0.2 \\ c_k = -65 \\ d_k = 8 \\ \\ D_{b,k} = 0.2 \\ c_k = -50 \\ d_k = 2 \end{array} \qquad 1 \leq k \leq N_a \\ N_a + 1 \leq k \leq N_a + N_c \\ N_a + 1 \leq k \leq N_a + N_a + N_c \\ N_a + 1 \leq k \leq N_a + N_a + N_c \\ N_a + 1 \leq k \leq N_a + N_a +$$

$$D_{b,k} = 0.05$$

 $c_k = -65$ $N_a + N_c + 1 \le k \le N$
 $d_k = 2$

and a being 0.02. The synaptic current I can be modeled by the sum of the fired neuron currents with the background current which represents the unmodeled electrical activity of the brain:

$$I = I_f + I_b \tag{4}$$

where $I_{f_k} = \sum s_{k,m}$, which $s_{k,m}$ represents the synaptic weight from the *m*-fired neuron connected to the *k*-neuron. Since the sum occurs for every neuron and overall fired neurons, the current I_f guarantees full connectivity among the neurons. The background current I_b is given by a normal distribution with null mean and standard deviation of 5, 5.1, and 1.3 to the PNa, PNc, and FSI neurons, respectively.

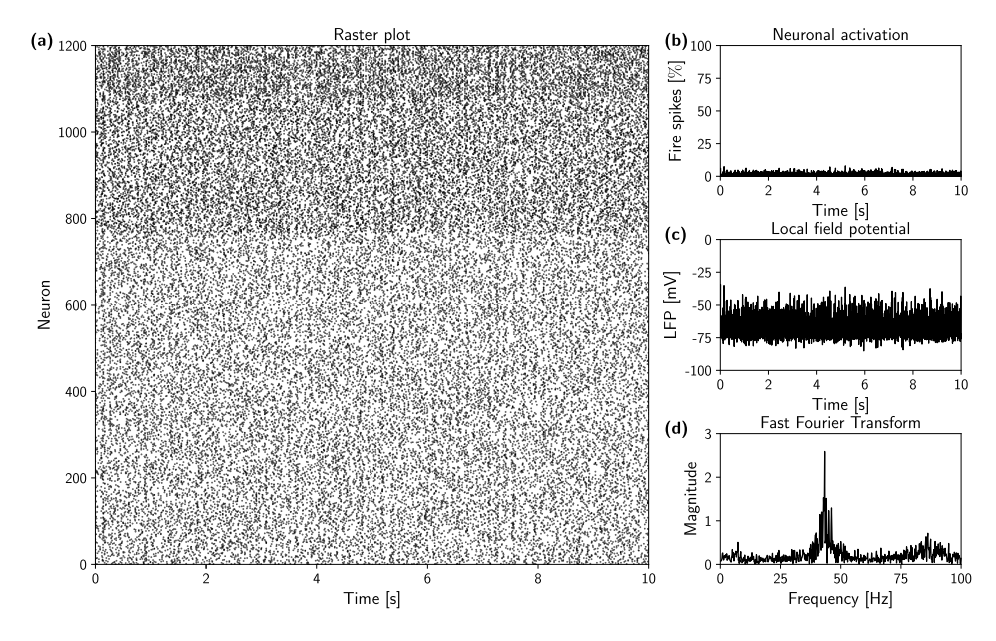


Fig. 3. Experiment showing a neuronal network in normal activity: the network does not present any signal of synchronous behavior. The maximum synaptic weights of each sub-population are defined as 0.5 for PNa and PNc, and -3.5 for FSI. From now on, the neurons on the raster plot are aligned following the sequence in the y-axis: rows 1 to 768 for PNa, 769 to 1080 for PNc, and 1081 to 1200 for FSI.

TABLE I
SYNAPTIC WEIGHTS USED TO INDUCE ICTOGENESIS

Case	PNa ₀	PNa∞	PNc_0	PNc_{∞}	FSI_0	FSI_{∞}
1	0.5	1	0.5	0.5	-3.5	-3.5
2	0.5	0.5	0.5	1	-3.5	-3.5
3	0.5	1	0.5	1	-3.5	-3.5
4	0.5	0.5	0.5	0.5	-3.5	0

The Fig. 3 shows the raster plot and the local field potential (LFP) of the neuronal model simulated as described above. The Euler method with time steps of 1 ms was employed to numerically solve the model (1)-(3) and simulate the neuronal population. The inject current was set to be null. The LFP was calculated by the weighted average of \boldsymbol{v} with weights obtained from a continuous uniform distribution:

$$LFP = \boldsymbol{\theta}^{\top} \boldsymbol{v} \tag{5}$$

Although there are other more sophisticated approaches for calculating the LFP of a network of neurons [45], [49], for our control purposes, the formula (5) is sufficient.

A. Induction of Ictogenesis

The process of ictogenesis was simulated by a gradual asymptotic modification of the synaptic weights to different values from what was initially set according to the cases described in the Table I. The rationale here is to tamper with the delicate balance between inhibition and excitation (in favor of the latter), which correlates to many of the neurolobiological mechanisms of ictogenesis. The update rule for the synaptic weights is given by integrating the first-order differential equation (6), with $\tau_p=1500$ and $p=\{\text{PNa, PNc, FSI}\}$. The initial condition is given by p_0 according to the Table I.

$$\dot{p} = \frac{p_{\infty} - p}{\tau_p} \tag{6}$$

The results shown in Fig. 4-5 are related to cases 1 to 4, respectively. It can be noted in all the raster plots that after a certain period of modification in the synaptic weight, a time that changes depending on the case and can reach up to approximately 2 seconds in case 2, the neurons exhibit synchronized firing behavior, which indicates that the substrate is displaying epileptiform activity, which would translate to an epileptic seizure when extrapolating the model. Notably, in case 2, the ictogenesis process does not start as abruptly as observed in other cases; instead, it begins gradually and subsequently exhibits a pattern similar to the remaining cases. This same behavior can be observed in the neural activation plot, which shows the percentage of firing neurons, and also by the LFP itself, which presents a typical behavior of a sharp and rhythmic rise in the membrane voltage level. Another point to be highlighted is that while in normal behavior the frequency spectrum, Fig. 3(d), indicates that the highest magnitude is present at a high frequency of approximately 40 Hz, a sign of the asynchronous activity of the network, in the cases where ictogenesis was induced, Fig. 4(d)-(h) and Fig. 5(d)-(h), the predominance of much lower frequencies is detected, such as approximately 4Hz in case 3, and the corresponding harmonics, a characteristic of the synchronized activity also observed in the other graphs.

The objective of the intelligent controller, presented in the next section, is to suppress such behavior and return the network to normal activity.

III. INTELLIGENT CONTROL

In principle, it would be possible to design the controller in such a way that it can track each neuron individually. However, such a task is impractical for at least two reasons: first, it would be necessary to know the isolated behavior of each neuron in order to calculate the correct signal for each one; and second,

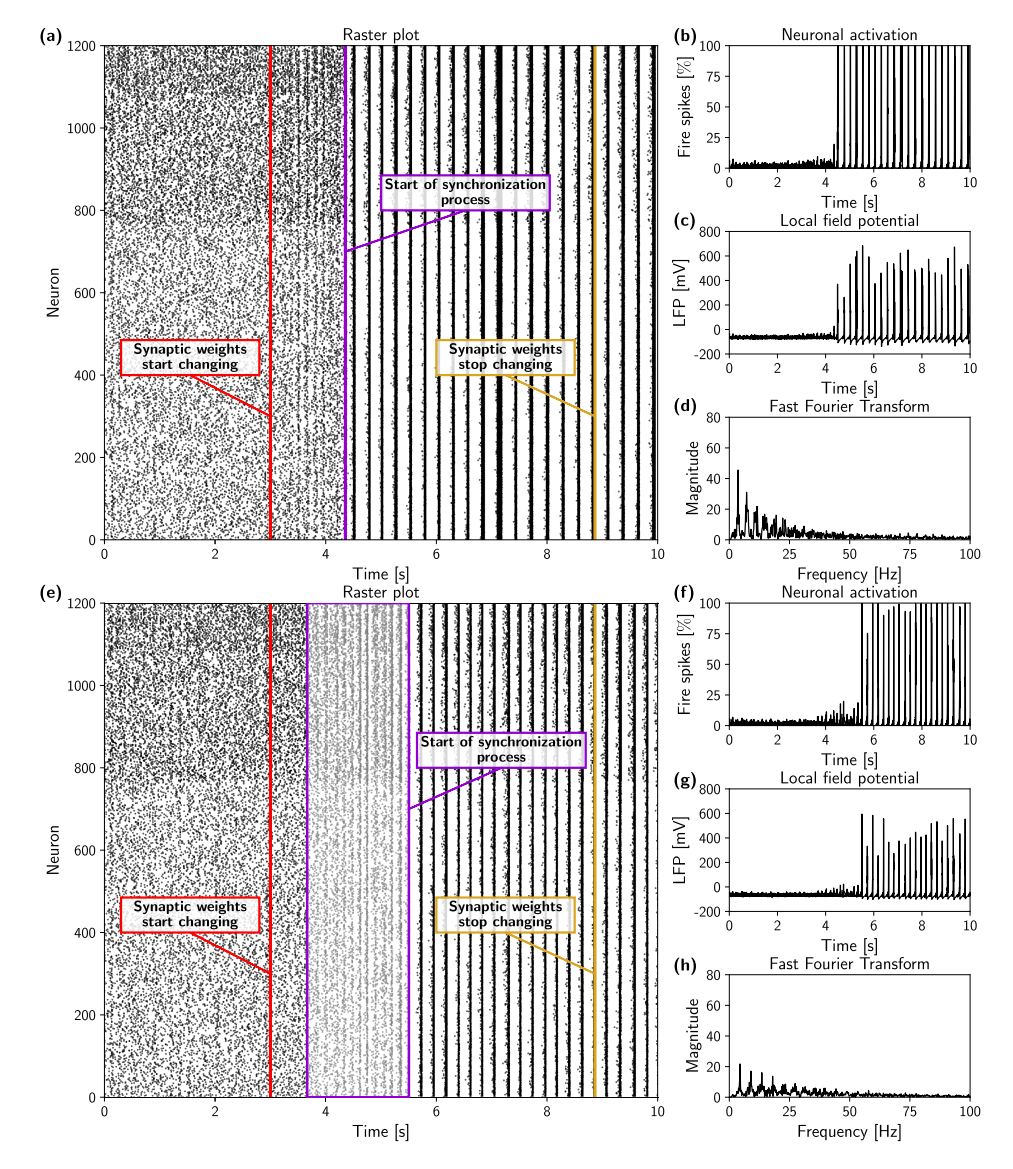


Fig. 4. Experiment for cases 1 (a-d) and 2 (e-h) showing a neuronal network in aberrant activity after the synaptic weights changed. In the case 1 and 2, the excitatory synaptic weights of PNa and PNc sub-populations were increased from 0.5 to 1, respectively. In both cases, the synchronous behavior starts after some seconds into process of changing the synaptic weights.

assuming the first reason was not an issue, it would be necessary for each neuron to be individually accessible, so that the necessary control effort could be assigned to it. To overcome this issue, it is first essential to identify the state variable capable of representing the overall behavior of the system. As observed in Fig. 3-5, the local field potential is a wellsuited variable to be used as a reference for the network state. Due to this, for the sole purpose of facilitating the derivation of a control law, the original model (1)-(3) is rewritten in a simplified form, ensuring that the overall network dynamics remain manageable. Therefore, consider that x is the Local Field Potential (or LFP), i.e. the electrographic oscillation resulting from the combined contributions of extracellular currents generated by the activity of each neuron in the network propagated across the volume conduction represented by the brain tissue. Then, by combining equations (5) and (1), we can express the global dynamics of the N-neuron network

in terms of LFP as follows:

$$\dot{x} = f(x, t) + \bar{J} + d \tag{7}$$

where the function $f = \boldsymbol{\theta}^{\top}[0.04 \ D_v \boldsymbol{v} + 5\boldsymbol{v} + 140 - \boldsymbol{u}]$ incorporates the internal dynamics of the system, \bar{J} is the control variable, and d aggregates the uncertainties the neglected dynamics associated with the simplification as well as the external disturbances. Since the control input for all neurons is encapsulated in the vector $\boldsymbol{J} \in \mathbb{R}^N$ from Eq. (1), each element J_i represents the control input for the i-th neuron and is computed as $J_i = \bar{\theta}_i \bar{J}$, where $\bar{\theta}_i$ represents the distance between the i-th neuron and the electrical stimulator. The values of $\bar{\theta}_i$ are weights drawn from a uniform distribution, i.e., $\bar{\theta}_i \in \mathcal{U}_{[0,1]}$.

In order to derive the control law, consider the positive-definite Lyapunov candidate function $V(t) = \frac{1}{2}\tilde{x}^2$, where $\tilde{x} = x - x_d$ is the tracking error with x_d being the desired

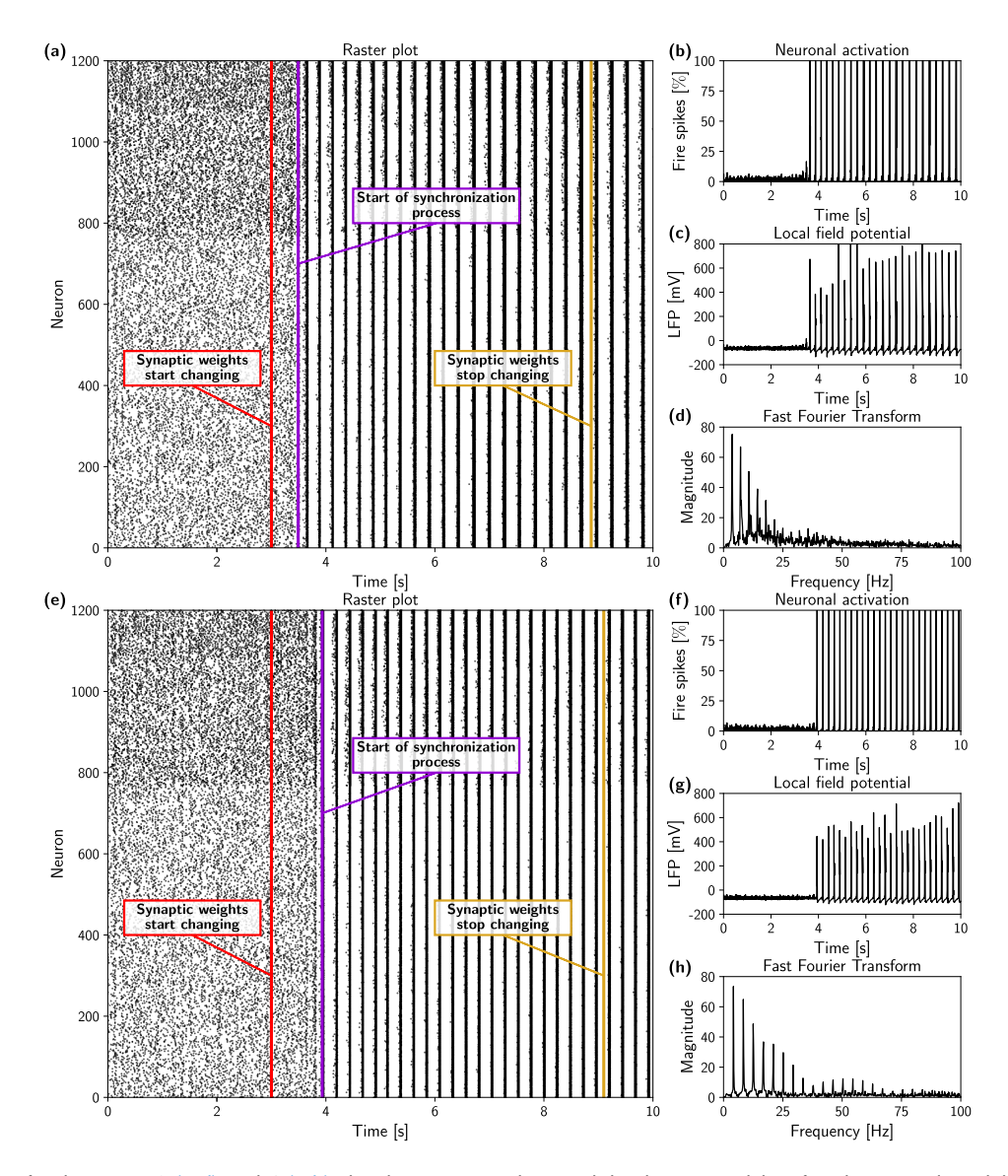


Fig. 5. Experiment for the cases 3 (a-d) and 4 (e-h) showing a neuronal network in aberrant activity after the synaptic weights changed. While in the case 3, the excitatory synaptic weights of PNa and PNc sub-populations were increased from 0.5 to 1, simultaneously, in the case 4, the inhibitory synaptic weights of FSI sub-population was decreased in magnitude (simulating less inhibition) from -3.5 to 0.

LFP. The first derivative of V becomes:

$$\dot{V}(t) = \tilde{x}\dot{\tilde{x}} = \tilde{x}[\dot{x} - \dot{x}_d]
= \tilde{x}[f + \bar{J} + d - \dot{x}_d]$$
(8)

Defining the control law by:

$$\bar{J} = -f - \hat{d} + \dot{x}_d - \lambda \tilde{x} \tag{9}$$

in which \hat{d} is the estimate of d and with λ being a positive constant, we have

$$\dot{V}(t) = \tilde{x}[d - \hat{d} - \lambda \tilde{x}] \tag{10}$$

Assuming that $|d - \hat{d}| \leq \varepsilon$, $\dot{V}(t)$ becomes a negative-definite function only when $|\tilde{x}| \geq \varepsilon/\lambda$. Therefore, a suitable \hat{d} is fundamental to guarantee the boundaries of the tracking error and, consequently, the structural stability in the sense of Lyapunov.

So, consider that a single-hidden layer artificial neural network, as depicted at the Fig. 6, can perform universal

approximation [50] and approximate the unknown dynamics:

$$\hat{d} = \boldsymbol{w}^{\top} \boldsymbol{\psi}(\tilde{x}) \tag{11}$$

where $\boldsymbol{w} = [w_1 \ldots w_n]^{\top}$ are the weights of the neural network and $\boldsymbol{\psi}(\tilde{x}) = [\psi_1 \ldots \psi_n]^{\top}$ the activation functions. It should be pointed out that by using the LFP error as input to the network, instead of the state of each Izhikevich neuron, the computational complexity exponentially decreases from n^N to n.

Admitting there is a vector of optimum weights $\bar{\boldsymbol{w}}$ that minimizes the approximation error $\epsilon = d - \bar{\boldsymbol{w}}^{\top} \boldsymbol{\psi}$, where $|\epsilon| \leq \varepsilon$, the candidate Lyapunov function can be modified as follows:

$$V(t) = \frac{1}{2}\tilde{x}^2 + \frac{1}{2\eta}\tilde{\boldsymbol{w}}^{\top}\tilde{\boldsymbol{w}}$$
 (12)

where η é a strictly positive constant and $\tilde{\boldsymbol{w}} = \bar{\boldsymbol{w}} - \boldsymbol{w}$.

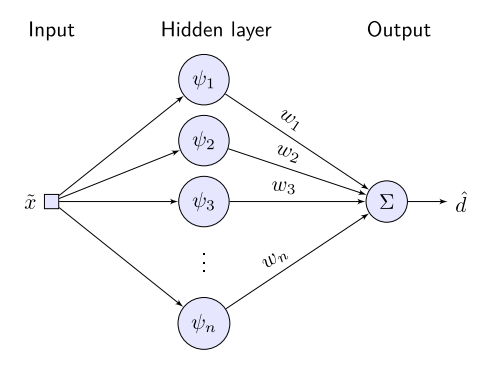


Fig. 6. Single-hidden layer network.

Computing the time derivative of V(t) and considering that $\dot{\tilde{w}} = -\dot{w}$, we have

$$\dot{V}(t) = \tilde{x}\dot{\tilde{x}} - \eta^{-1}\tilde{\mathbf{w}}^{\top}\dot{\mathbf{w}} = \tilde{x}[d - \hat{d} - \lambda\tilde{x}] - \eta^{-1}\tilde{\mathbf{w}}^{\top}\dot{\mathbf{w}}
= \tilde{x}[\bar{\mathbf{w}}^{\top}\mathbf{\psi} - \mathbf{w}^{\top}\mathbf{\psi} + \epsilon - \lambda\tilde{x}] - \eta^{-1}\tilde{\mathbf{w}}^{\top}\dot{\mathbf{w}}
= \tilde{x}[\tilde{\mathbf{w}}^{\top}\mathbf{\psi} + \epsilon - \lambda\tilde{x}] - \eta^{-1}\tilde{\mathbf{w}}^{\top}\dot{\mathbf{w}}
= \tilde{x}[\epsilon - \lambda\tilde{x}] - \eta^{-1}\tilde{\mathbf{w}}^{\top}[\dot{\mathbf{w}} - \eta\tilde{x}\mathbf{\psi}]$$
(13)

By definition of the adaption law for the neural weights as

$$\dot{\boldsymbol{w}} = \eta \tilde{\boldsymbol{x}} \boldsymbol{\psi} \tag{14}$$

the first derivative of V(t) becomes,

$$\dot{V}(t) = -[\lambda \tilde{x} - \epsilon]\tilde{x} \le -[\lambda |\tilde{x}| - \epsilon]|\tilde{x}| \tag{15}$$

It should be noted that equation (15) does not guarantee that $\|\boldsymbol{w}\|_2$ will be bounded when $|\tilde{x}| \leq \varepsilon/\lambda$. To address this issue, the projection algorithm [51] can be used to ensure that \boldsymbol{w} will remain within the region $\mathcal{W} = \{\boldsymbol{w} \in \mathbb{R}^n : \boldsymbol{w}^\top \boldsymbol{w} \leq \mu^2\}$:

$$\dot{\boldsymbol{w}} = \begin{cases} \eta \tilde{\boldsymbol{x}} \boldsymbol{\psi} & \text{if } \|\boldsymbol{w}\|_{2} < \mu \text{ or} \\ & \text{if } \|\boldsymbol{w}\|_{2} = \mu \text{ and } \eta \tilde{\boldsymbol{x}} \boldsymbol{w}^{\top} \boldsymbol{\psi} < 0 \\ \left(\boldsymbol{I} - \frac{\boldsymbol{w} \boldsymbol{w}^{\top}}{\boldsymbol{w}^{\top} \boldsymbol{w}}\right) \eta \tilde{\boldsymbol{x}} \boldsymbol{\psi} & \text{otherwise} \end{cases}$$
(16)

where μ is the desired upper limit of $\|\boldsymbol{w}\|_2$ and η will be called the learning rate of the neural network.

Since $\|\boldsymbol{w}(0)\|_2 \leq \mu$, it follows that $|\tilde{x}| \leq \varepsilon/\lambda$ and that $\|\boldsymbol{w}\|_2 \leq \mu$ as $t \to \infty$, which guarantees that the controller will ensure the exponential convergence of the tracking error to a closed region [52]. The control framework is illustrated in Fig. 7.

IV. SIMULATION RESULTS

The controller was employed with time steps of 5 ms and control parameter set to be $\lambda=0.01$. Additionally, by defining f=0, we are imposing that the control designer has no prior knowledge about the system dynamics, so we rely on that the ANN will compensate for it while simultaneously dealing with the external disturbances and addressing various epileptiform scenarios, which ultimately represent independent cases of different patients. It is important to note that the controller without ANN was tested first.

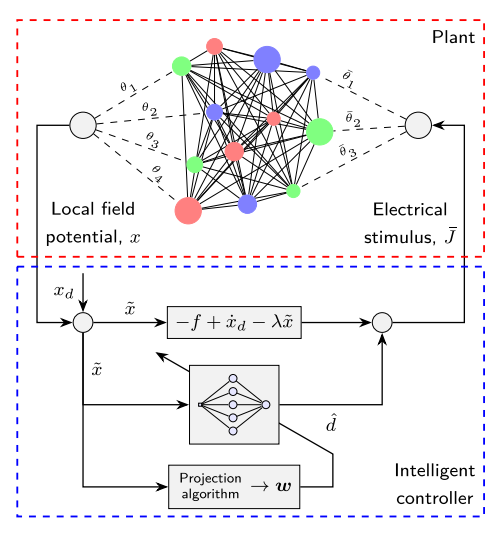


Fig. 7. Controller framework with the representation of how the computed electrical stimulus is applied to the Izhikevich network (the indices are for illustrative purposes).

but the outcomes were unsatisfactory, as the controller did not suppress the epileptic seizures. So, regarding the neural network, six neurons were adopted with Gaussian activation functions: $\psi_i(\tilde{x}; c_i, \gamma_i) = \exp\{-0.5[(\tilde{x} - c_i)/\gamma_i]^2\}$; with centers $\mathbf{c} = [-\phi, -\phi/2, -\phi/4, \phi/4, \phi/2, \phi]^{\top}$ and widths $\mathbf{\gamma} = [\phi/2, \phi/3, \phi/4, \phi/4, \phi/3, \phi/2]^{\top}$, for $\phi = 30$. Considering that the only restriction for the learning rate is that it must be a nonzero positive number and that increasing its value can increase the overall control effort, different values of η were tested in order to evaluate its optimum value. The results of the ANN output are shown in Fig. 8. The learning process occurs during 15 seconds of simulation after the start of the ictogenesis process.

It notes by observing the Fig. 8 that we have a convergence of the neural output after the learning rate of $\eta = 5 \times 10^{-4}$. The results with this learning rate are shown at the Fig. 9-10.

For case 1, it can be observed that although the controller is turned on at the instant of 10 seconds, the effect of desynchronization starts only around 12 seconds, as shown in Fig. 9(a). This is characterized by a drastic reduction in the proportion of firing neurons, Fig. 9(b), and a reduction in the LFP to the pre-ictogenesis stage, Fig. 9(c). This delay is due to the necessary time for the ANN to learn the system dynamics. It is also observed that the Fast Fourier Transform (FFT) shown in Fig. 9(e) indicates a dominant frequency close to the normal case of approximately 40 Hz, Fig. 3(d).

For the other cases a similar analysis can be made. While in case 2 the controller responds almost immediately, in case 4, where the neural network is in an excitatory process by reducing the inhibitory synaptic weights, the controller takes approximately 6 seconds to respond. However, in all cases, the controller proves to be effective in suppressing seizures, indicating a drastic reduction in the proportion of firing neurons and consequently a reduction in the LFP. Additionally, there is a return of the dominant frequency in the Fourier spectrum to a level around 40 Hz.

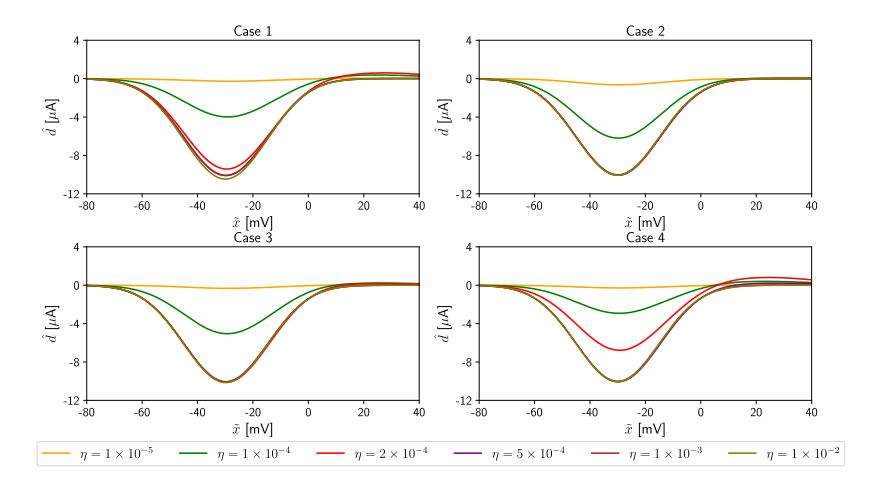


Fig. 8. Neural network output for different learning rates.

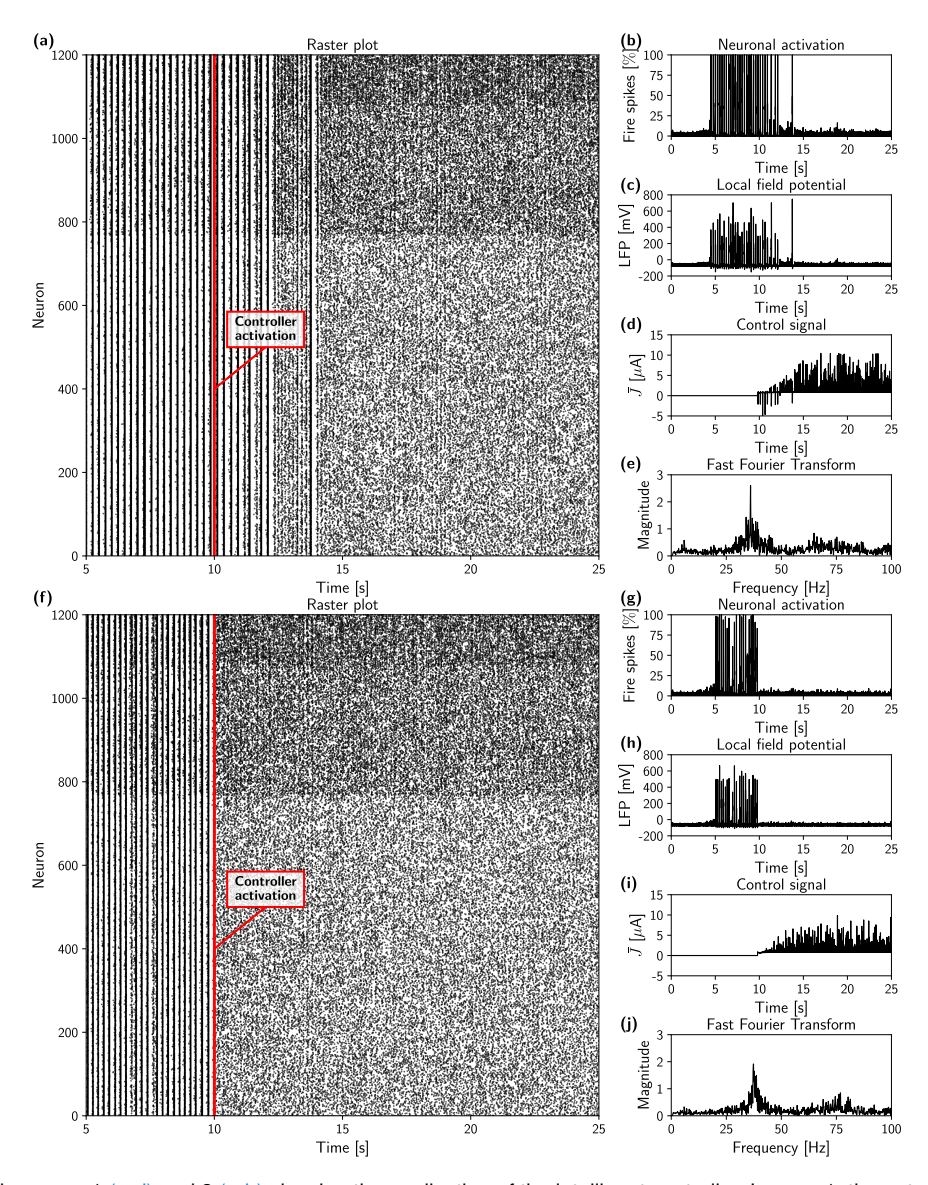


Fig. 9. Simulation for the cases 1 (a-d) and 2 (e-h) showing the application of the intelligent controller. In case 1, the network takes approximately 2 seconds to respond to the controller and return to normal behavior, which is observed not only in the raster plot, but also in the spiking rate and in the LFP. The same type of response is obtained in case 2, with the difference that the controller rapidly suppresses the ictogenesis process.

It is worth mentioning that even with a low learning rate, the ANN continuously approximate the neuronal dynamic as well

as compensate for the background current, which changes in each simulation loop for all cases. By doing so, the intelligent

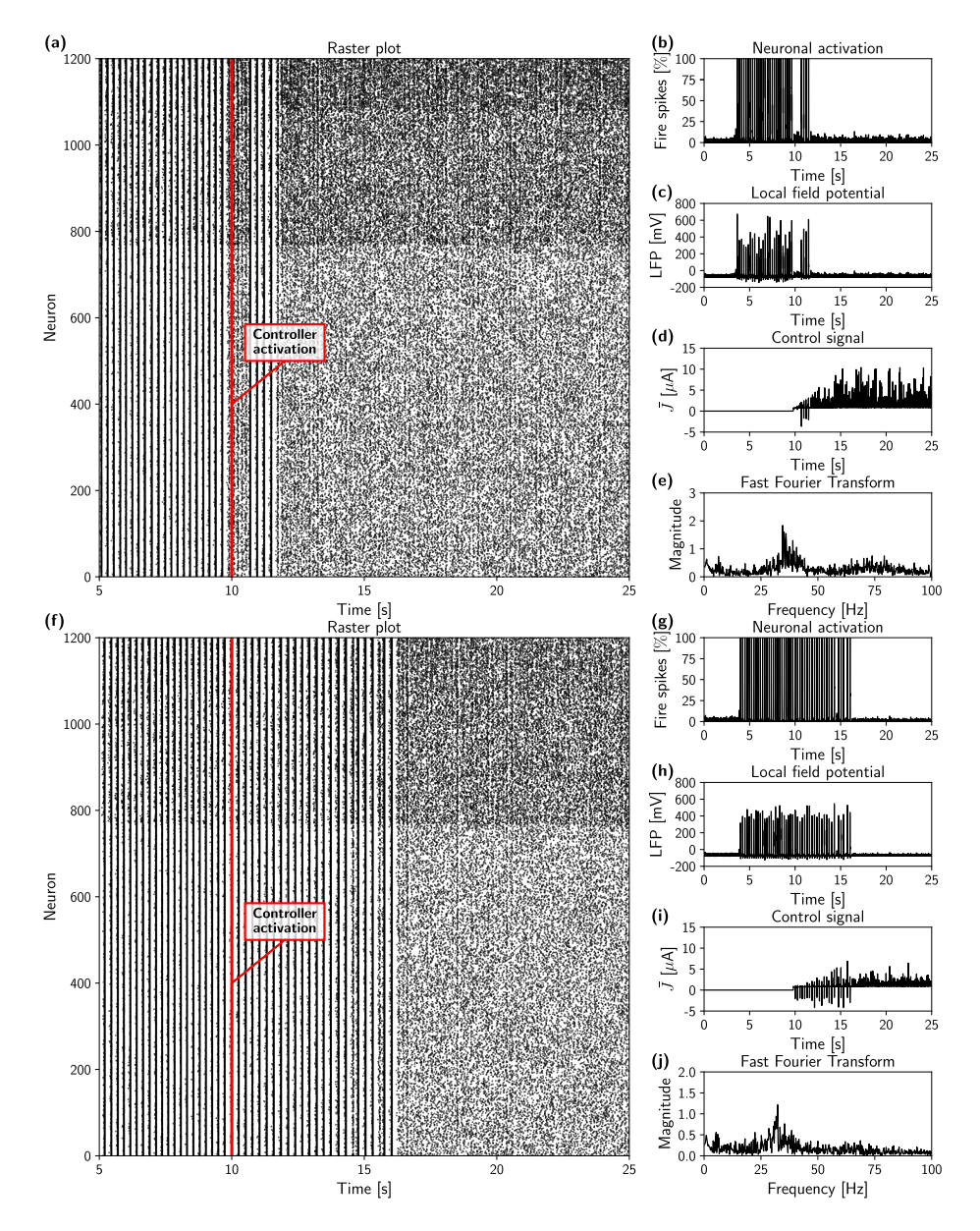


Fig. 10. Simulation for the cases 3 (a-d) and 4 (e-h) showing the application of the intelligent controller. In case 3, the network takes approximately 1 second to be stabilized by the controller and to return to normal behavior, which is observed in the raster plot, in the spiking rate, and in the LFP. The same type of response is obtained in case 4, with the difference that the controller needs 6 seconds to suppress the ictogenesis process.

controller demonstrates its capability to deal with external disturbances once the ANN stabilizes the approximation error.

V. CONCLUSION

In this work, we proposed an intelligent controller to suppress the aberrant activity of a network of Izhikevich neurons used to emulate the electrical activity typical of epileptic seizures. By using a computational model to represent the epileptiform activity of a network of interconnected neurons, we evaluated its ability to respond in real time to electrical stimulation and assessed the controller's performance in modulating the ongoing dynamics. The controller is based on a control scheme deduced by means of a Lyapunov-like

stability analysis, with artificial neural networks embedded into it to approximate and compensate for unknown dynamics and external disturbances, such as the external activity from the amygdala's surrounding areas. The choice for the adopted neural network decreased the computational complexity, making it possible to implement it in hardware devices. To bypass the issue of targeting each neuron individually, the LFP was used to represent the entire network's state and the electrical stimulation for each neuron was computed to be proportional to the main control signal. The presented results demonstrate the effectiveness of intelligent controllers in suppressing aberrant neural activity, even when the controller operates without considering any prior information about the patient's neural behavior.

It should be emphasized that epilepsy is a multi-faceted phenomenon involving factors in multiple levels of brain organization, from molecules to cells, to micro-circuits, and finally to mid and long-range networks [43]. Adding to its complexity, the epilepsy phenomena also encompasses nonneuronal factors, such as glial and cardiovascular dysfunction. For this reason, any brain tissue and seizure model will be reductionist to a certain extent - or highly abstract, such as the Epileptor model [40]. In this work, a network of Izhikevich neurons was used to model the basolateral nucleus of the amygdaloid complex, which plays a crucial role in epileptic phenomena and neuromodulation treatments [42], [43]. In many different aspects, it can be considered even more important than the hippocampus itself [53]. Furthermore, this model has been shown to be instrumental for investigating neural synchronization, phase transitions, the pathophysiology of the disease, as well as the effects of therapeutical approaches such as neurostimulation [12], [38], [44], [45], [46], [48], [54]. Overall, our choice of this model represented a balance between computational feasibility and biological plausibility, ensuring a representation realistic enough for the main purpose of this study: investigating the feasibility of the intelligent controllers.

In our study, the efficacy of the controller in suppressing hypersynchronization was evaluated across different scenarios, where epileptiform activity was induced using four distinct strategies (modifications of various synaptic weights). In all tested cases, the intelligent controller successfully returned the Izhikevich network to an asynchronous pattern, indicating its potential to provide improved solutions for closed-loop neurotechnologies. This is particularly relevant because seizures can vary significantly not only across epilepsies of different etiologies but also between patients and even over time in the same individual (e.g., during kindling processes). Therefore, the present results support the use of intelligent controllers as effective tools for managing this neurological disorder.

Additionally, two points regarding the controller should be addressed. First, although the control scheme is continuous, it should not be interpreted as a literal DC current, as this could potentially cause neural tissue damage. Instead, it represents a continuous effort to modulate excitability (either increasing or decreasing), which can be achieved in real settings through charge-balanced pulsatile stimulation. In this sense, consolidated neurostimulation medical devices, such as those used in DBS of the thalamus or VNS, employ stimulation protocols that continuously alternate between ON and OFF stimulation periods spanning many days, even weeks and even months uninterruptedly. Yet, they provide safe and effective treatment that is well tolerated by patients. Furthermore, it is well established in the neurostimulation literature that charge-balanced electrical stimulation of brain tissue, when parameters are kept within safe ranges, poses no substantial lesion risk, causes minimal to no adverse effects, and can even improve neural function in some cases [55], [56], [57].

Secondly, it is important to consider the perspective that algorithms for seizure detection and prediction [58], [59] should be incorporated into controllers such as the one presented here for optimal functioning. While the latter is still

considered as an unresolved issue [60] when evaluated using more rigorous statistical frameworks [61], [62], the former has in fact been used in state-of-the-art seizure-suppressing responsive neurotecnologies, such as RNS from Neuropace (REF). Yet, this does not preclude the advantages of using intelligent controllers. In this case, they may serve at least two complementary objectives: a) as a detector to respond in realtime to impending seizures and, b) as an optimizer to deliver minimal efficacious levels of electrical stimulation. Furthermore, although not explicitly tested here, once the controller output is directly dependent on the presence of epileptiform spikes, it is plausible that stimuli intensity would be very low or non-existent during inter-ictal (between seizures or during absence of spikes) periods. Finally, one can choose more sophisticated methods for the detection of abnormal neural activity as the input of the controller, including those sensible to very minor deviations from healthy neuronal dynamics, maybe even putative seizure prediction algorithms. In these cases, intelligent controllers such as the present one would be optimal as they would respond with minimal intervention in the form of preemptive stimulation capable of restoring healthy oscillatory patterns and thus prevent seizures from even begging. In any case, such promising and intriguing technological and scientific perspectives can be certainly pursued with the employment of intelligent controllers.

Naturally, further studies are essential to more definitively establish intelligent strategies such as ours as effective for seizure control. For instance, refining the neural tissue and ictogenesis models, as well as enhancing the interface model for generating LFP signals and simulating stimulation effects, would benefit interpretability while also enhancing biological plausibility of simulations. Specifically, converting the current quasi-continuous control signals into rhythmic pulsed electrical stimulation is necessary to better replicate real neurostimulation scenarios is crucial. Additionally, comparing simulation results with clinical data and conducting preclinical trials are natural and vital steps in this line of investigation. These efforts are mandatory to validating the proposed control strategies and ensuring their translational potential. As part of our future plans, we aim to implement the enhanced controller in animal models of epilepsy and evaluate its efficacy in scenarios more closely aligned with clinical practice.

REFERENCES

- [1] J. H. Chin and N. Vora, "The global burden of neurologic diseases," *Neurology*, vol. 83, no. 4, pp. 349–351, Feb. 2014.
- [2] V. L. Feigin et al., "The global burden of neurological disorders: Translating evidence into policy," *Lancet Neurol.*, vol. 19, no. 3, pp. 255–265, Mar. 2020.
- [3] J. Murphy et al., "Variation in access to specialist services for neurosurgical procedures in adults with epilepsy in England, a cohort study," *Seizure*, vol. 116, pp. 140–146, Mar. 2022.
- [4] C. Granthon, A. E. Tranberg, K. Malmgren, M. C. Strandberg, E. Kumlien, and P. Redfors, "Reduced long-term mortality after successful resective epilepsy surgery: A population-based study," *J. Neurol.*, *Neurosurg. Psychiatry*, vol. 95, no. 3, pp. 249–255, Mar. 2024.
- [5] J. Engel, Epilepsy: Global Issues for the Practicing Neurologist, vol. 2. New York, NY, USA: Demos Medical Publishing, 2005.
- [6] N. Savage, "Epidemiology: The complexities of epilepsy," *Nature*, vol. 511, no. 7508, pp. S2–S3, Jul. 2014.

- [7] V. R. Cota, S. A. V. Cançado, and M. F. D. Moraes, "On temporal scale-free non-periodic stimulation and its mechanisms as an infinite improbability drive of the brain's functional connectogram," *Frontiers Neuroinform.*, vol. 17, May 2023, Art. no. 1173597.
- [8] M. Chiappalone et al., "Neuromorphic-based neuroprostheses for brain rewiring: State-of-the-art and perspectives in neuroengineering," *Brain Sci.*, vol. 12, no. 11, p. 1578, Nov. 2022.
- [9] K. K. Sellers et al., "Closed-loop neurostimulation for the treatment of psychiatric disorders," *Neuropsychopharmacology*, vol. 49, no. 1, pp. 163–178, Jan. 2024.
- [10] N. L. Opie and T. J. O'Brien, "The potential of closed-loop endovascular neurostimulation as a viable therapeutic approach for drug-resistant epilepsy: A critical review," *Artif. Organs*, vol. 46, no. 3, pp. 337–348, Mar. 2022.
- [11] D. A. Wagenaar, R. Madhavan, J. Pine, and S. M. Potter, "Controlling bursting in cortical cultures with closed-loop multi-electrode stimulation," *J. Neurosci.*, vol. 25, no. 3, pp. 680–688, Jan. 2005.
- [12] G. D. S. Lima, V. R. Cota, and W. M. Bessa, "In silico application of the epsilon-greedy algorithm for frequency optimization of electrical neurostimulation for hypersynchronous disorders," in *Proc. Latin Amer. Workshop Comput. Neurosci.*, Cham, Switzerland. Springer, 2023, pp. 57–68.
- [13] Z. Liang, Z. Luo, K. Liu, J. Qiu, and Q. Liu, "Online learning Koopman operator for closed-loop electrical neurostimulation in epilepsy," *IEEE J. Biomed. Health Informat.*, vol. 27, no. 1, pp. 492–503, Jan. 2022.
- [14] E. Rouhani, E. Jafari, and A. Akhavan, "Suppression of seizure in child-hood absence epilepsy using robust control of deep brain stimulation: A simulation study," Sci. Rep., vol. 13, no. 1, p. 461, Jan. 2023.
- [15] M. Koppert, S. Kalitzin, D. Velis, F. Lopes Da Silva, and M. A. Viergever, "Preventive and abortive strategies for stimulation based control of epilepsy: A computational model study," *Int. J. Neural Syst.*, vol. 26, no. 8, Dec. 2016, Art. no. 1650028.
- [16] A. Berényi, M. Belluscio, D. Mao, and G. Buzsáki, "Closed-loop control of epilepsy by transcranial electrical stimulation," *Science*, vol. 337, no. 6095, pp. 735–737, Aug. 2012.
- [17] N. Muthiah et al., "Comparison of traditional and closed loop vagus nerve stimulation for treatment of pediatric drug-resistant epilepsy: A propensity-matched retrospective cohort study," *Seizure*, vol. 94, pp. 74–81, Jan. 2022.
- [18] R. V. Mylavarapu, V. V. Kanumuri, J. P. de Rivero Vaccari, A. Misra, D. W. Mcmillan, and P. D. Ganzer, "Importance of timing optimization for closed-loop applications of vagus nerve stimulation," *Bioelectron. Med.*, vol. 9, no. 1, pp. 1–8, Apr. 2023.
- [19] D. N. Anderson et al., "Closed-loop stimulation in periods with less epileptiform activity drives improved epilepsy outcomes," *Brain*, vol. 147, no. 2, pp. 521–531, 2024.
- [20] S. Ovadia-Caro, A. A. Khalil, B. Sehm, A. Villringer, V. V. Nikulin, and M. Nazarova, "Predicting the response to noninvasive brain stimulation in stroke," *Frontiers Neurol.*, vol. 10, p. 302, Apr. 2019.
- [21] M. Carè, M. Chiappalone, and V. R. Cota, "Personalized strategies of neurostimulation: From static biomarkers to dynamic closed-loop assessment of neural function," *Frontiers Neurosci.*, vol. 18, Mar. 2024, Art. no. 1363128.
- [22] W. M. Bessa, E. Kreuzer, J. Lange, M.-A. Pick, and E. Solowjow, "Design and adaptive depth control of a micro diving agent," *IEEE Robot. Autom. Lett.*, vol. 2, no. 4, pp. 1871–1877, Oct. 2017.
- [23] G. S. Lima, S. Trimpe, and W. M. Bessa, "Sliding mode control with Gaussian process regression for underwater robots," *J. Intell. Robotic Syst.*, vol. 99, no. 3, pp. 487–498, Sep. 2020.
- [24] D. Zhu, S. X. Yang, and M. Biglarbegian, "A fuzzy logic-based cascade control without actuator saturation for the unmanned underwater vehicle trajectory tracking," *J. Intell. Robotic Syst.*, vol. 106, no. 2, p. 39, Oct. 2022.
- [25] G. da Silva Lima, V. R. F. Moreira, and W. M. Bessa, "Accurate trajectory tracking control with adaptive neural networks for omnidirectional mobile robots subject to unmodeled dynamics," *J. Brazilian Soc. Mech. Sci. Eng.*, vol. 45, no. 1, p. 48, Jan. 2023.
- [26] P. V. G. Simplício, J. R. S. Benevides, R. S. Inoue, and M. H. Terra, "Robust and intelligent control of quadrotors subject to wind gusts," *IET Control Theory Appl.*, vol. 18, no. 18, pp. 2594–2611, Dec. 2024.
- [27] W. M. Bessa, S. Otto, E. Kreuzer, and R. Seifried, "An adaptive fuzzy sliding mode controller for uncertain underactuated mechanical systems," J. Vibrat. Control, vol. 25, no. 9, pp. 1521–1535, May 2019.

- [28] G.-L. Guo, C.-M. Lin, H.-Y. Cho, D.-H. Pham, T.-T. Huynh, and F. Chao, "Decoupled sliding mode control of underactuated nonlinear systems using a fuzzy brain emotional cerebellar model control system," *Int. J. Fuzzy Syst.*, vol. 25, no. 1, pp. 15–28, Feb. 2023.
- [29] X. Zeng and D. Wang, "Optimal tracking control of the coal mining face fluid supply system via adaptive dynamic programming," Sci. Rep., vol. 13, no. 1, p. 20002, Nov. 2023.
- [30] M. Abdillah, E. M. Mellouli, and T. Haidi, "A new intelligent controller based on integral sliding mode control and extended state observer for nonlinear MIMO drone quadrotor," *Int. J. Intell. Netw.*, vol. 5, pp. 49–62, Jan. 2024.
- [31] B. Zhang, P. Niu, X. Guo, and J. He, "Fuzzy PID control of permanent magnet synchronous motor electric steering engine by improved beetle antennae search algorithm," Sci. Rep., vol. 14, no. 1, p. 2898, Feb. 2024.
- [32] H. Benbouhenni, G. Hamza, M. Oproescu, N. Bizon, P. Thounthong, and I. Colak, "Application of fractional-order synergetic-proportional integral controller based on PSO algorithm to improve the output power of the wind turbine power system," Sci. Rep., vol. 14, no. 1, p. 609, Jan. 2024.
- [33] M. E. Karar, "Robust RBF neural network-based backstepping controller for implantable cardiac pacemakers," *Int. J. Adapt. Control Signal Process.*, vol. 32, no. 7, pp. 1040–1051, Jul. 2018.
- [34] G. S. Lima, M. A. Savi, and W. M. Bessa, "Intelligent control of cardiac rhythms using artificial neural networks," *Nonlinear Dyn.*, vol. 111, no. 12, pp. 11543–11557, Jun. 2023.
- [35] J. L. C. B. de Farias and W. M. Bessa, "Intelligent control with artificial neural networks for automated insulin delivery systems," *Bioengineer*ing, vol. 9, no. 11, p. 664, Nov. 2022.
- [36] S. N. Narayanan and S. Subbian, "HH model based smart deep brain stimulator to detect, predict and control epilepsy using machine learning algorithm," J. Neurosci. Methods, vol. 389, Apr. 2023, Art. no. 109825.
- [37] W. M. Bessa and G. D. S. Lima, "Intelligent control of seizure-like activity in a memristive neuromorphic circuit based on the Hodgkin– Huxley model," *J. Low Power Electron. Appl.*, vol. 12, no. 4, p. 54, Oct. 2022.
- [38] E. M. Izhikevich, "Which model to use for cortical spiking neurons?" IEEE Trans. Neural Netw., vol. 15, no. 5, pp. 1063–1070, Sep. 2004.
- [39] J. A. F. Brogin, J. Faber, and D. D. Bueno, "An efficient approach to define the input stimuli to suppress epileptic seizures described by the epileptor model," *Int. J. Neural Syst.*, vol. 30, no. 11, Nov. 2020, Art. no. 2050062.
- [40] V. K. Jirsa, W. C. Stacey, P. P. Quilichini, A. I. Ivanov, and C. Bernard, "On the nature of seizure dynamics," *Brain*, vol. 137, no. 8, pp. 2210–2230, Aug. 2014.
- [41] W. M. Bessa, G. Brinkmann, D. A. Duecker, E. Kreuzer, and E. Solowjow, "A biologically inspired framework for the intelligent control of mechatronic systems and its application to a micro diving agent," *Math. Problems Eng.*, vol. 2018, Dec. 2018, Art. no. 9648126.
- [42] V. R. Cota, D. D. C. Medeiros, M. R. S. D. P. Vilela, M. C. Doretto, and M. F. D. Moraes, "Distinct patterns of electrical stimulation of the basolateral amygdala influence pentylenetetrazole seizure outcome," *Epilepsy Behav.*, vol. 14, no. 1, pp. 26–31, Jan. 2009.
- [43] V. R. Cota, B. M. B. Drabowski, J. C. de Oliveira, and M. F. D. Moraes, "The epileptic amygdala: Toward the development of a neural prosthesis by temporally coded electrical stimulation," *J. Neurosci. Res.*, vol. 94, no. 6, pp. 463–485, Jun. 2016.
- [44] E. M. Izhikevich, "Simple model of spiking neurons," *IEEE Trans. Neural Netw.*, vol. 14, no. 6, pp. 1569–1572, Nov. 2003.
- [45] J. P. S. E. Oliveira et al., "In silico investigation of the effects of distinct temporal patterns of electrical stimulation to the amygdala using a network of Izhikevich neurons," in *Proc. Latin Amer. Workshop Comput. Neurosci.*, Cham, Switzerland. Springer, 2021, pp. 132–152.
- [46] F. Feng et al., "Gamma oscillations in the basolateral amygdala: Biophysical mechanisms and computational consequences," *Eneuro*, vol. 6, no. 1, pp. 1–24, Jan. 2019.
- [47] M. J. Rubinow et al., "Basolateral amygdala volume and cell numbers in major depressive disorder: A postmortem stereological study," *Brain Struct. Function*, vol. 221, no. 1, pp. 171–184, Jan. 2016.
- [48] R. F. Pena, M. A. Zaks, and A. C. Roque, "Dynamics of spontaneous activity in random networks with multiple neuron subtypes and synaptic noise: Spontaneous activity in networks with synaptic noise," *J. Comput. Neurosci.*, vol. 45, pp. 1–28, Aug. 2018.
- [49] B. Telenczuk, M. Telenczuk, and A. Destexhe, "A kernel-based method to calculate local field potentials from networks of spiking neurons," *J. Neurosci. Methods*, vol. 344, Oct. 2020, Art. no. 108871.

- [50] F. Scarselli and A. C. Tsoi, "Universal approximation using feedforward neural networks: A survey of some existing methods, and some new results," *Neural Netw.*, vol. 11, no. 1, pp. 15–37, Jan. 1998.
- [51] P. Ioannou and B. Fidan, Adaptive Control Tutorial. Philadelphia, PA, USA: SIAM, 2006.
- [52] W. M. Bessa, "Some remarks on the boundedness and convergence properties of smooth sliding mode controllers," *Int. J. Autom. Comput.*, vol. 6, no. 2, pp. 154–158, May 2009.
- [53] E. M. Prager, G. H. Wynn, and R. J. Ursano, "The tenth annual amygdala, stress, and ptsd conference:," *J. Neurosci. Res.*, vol. 94, no. 6, pp. 433–436, 2016.
- [54] S. Hojjatinia, M. A. Shoorehdeli, Z. Fatahi, Z. Hojjatinia, and A. Haghparast, "Improving the Izhikevich model based on rat basolateral amygdala and hippocampus neurons, and recognizing their possible firing patterns," *Basic Clin. Neurosci.*, vol. 11, no. 1, p. 79, 2020.
- [55] M. C. Creed, C. Hamani, and J. N. Nobrega, "Effects of repeated deep brain stimulation on depressive- and anxiety-like behavior in rats: Comparing entopeduncular and subthalamic nuclei," *Brain Stimulation*, vol. 6, no. 4, pp. 506–514, Jul. 2013.
- [56] C. S. Inman et al., "Direct electrical stimulation of the amygdala enhances declarative memory in humans," *Proc. Nat. Acad. Sci. USA*, vol. 115, no. 1, pp. 98–103, Jan. 2018.

- [57] L. A. Réboli, R. M. Maciel, J. C. de Oliveira, M. F. D. Moraes, C. Q. Tilelli, and V. R. Cota, "Persistence of neural function in animals submitted to seizure-suppressing scale-free nonperiodic electrical stimulation applied to the amygdala," *Behav. Brain Res.*, vol. 426, May 2022, Art. no. 113843.
- [58] P. Luckett, E. Pavelescu, T. McDonald, L. Hively, and J. Ochoa, "Predicting state transitions in brain dynamics through spectral difference of phase-space graphs," *J. Comput. Neurosci.*, vol. 46, no. 1, pp. 91–106, Feb. 2019.
- [59] Z. Yang, D. Fan, Q. Wang, and G. Luan, "Sharp decrease in the Laplacian matrix rank of phase-space graphs: A potential biomarker in epilepsy," *Cognit. Neurodyn.*, vol. 15, no. 4, pp. 649–659, Aug. 2021.
- [60] M. O. Baud et al., "Seizure forecasting: Bifurcations in the long and winding road," *Epilepsia*, vol. 64, no. S4, pp. S78–S98, Dec. 2023.
- [61] F. Mormann, R. G. Andrzejak, C. E. Elger, and K. Lehnertz, "Seizure prediction: The long and winding road," *Brain*, vol. 130, no. 2, pp. 314–333, Feb. 2007.
- [62] D. R. Freestone et al., "Seizure prediction: Science fiction or soon to become reality?" *Current Neurol. Neurosci. Rep.*, vol. 15, no. 11, pp. 1–9, Nov. 2015.